MASTER'S THESIS

Master of Science in Advanced Mathematics and Mathematical Engineering

Title: Optimal coordinated motions for two square robots

Author: Víctor Ruiz Herrero

Advisor: Vera Sacristan, Rodrigo I. Silveira

Department: Applied mathematics

Academic year: 2019

UNIVERSITAT POLITÈCNICA DE CATALUNYA
BARCELONATECH
Facultat de Matemàtiques i Estadística

Universitat Politècnica de Catalunya
Facultat de Matemàtiques i Estadística

Master in Advanced Mathematics and Mathematical Engineering

Master's thesis

Optimal coordinated motions for two square robots

Víctor Ruiz Herrero

Supervised by Vera Sacristán, Rodrigo I. Silveira

September, 2019

Contents

Chapter 1

Introduction

Nowadays, with the high development of new technologies and artificial intelligence, robotics is a very important field of research. From electrical and mechanical engineering to computer science and applied mathematics, it covers plenty of many interesting subjects to study. In the general area of applied mathematics, this thesis treats a specific area of discrete mathematics and algorithmics, which is called computational geometry. The goal of computational geometry is the design of algorithms to solve geometric problems. Many types of computational geometry problems arise from robotics, concerning physical objects moving in the space or in the plane. The most important application of computational geometry to robotics is probably *motion planning*, and it is also a very natural and intuitive subject to work with.

Motion planning is an active field of research. It consists in producing a continuous motion that connects a start configuration of a robot (or a group of robots) and a goal configuration. Motion planning deals with many different aspects: determining feasibility of motion problems with obstacles for one or more robots, determining valid paths in an environment filled with obstacles, approximating the shortest path for a robot, determining paths in discrete grid problems etc. These problems and different approaches to solve motion planning problems are studied in [7] and many other books, journal and conference papers.

Our work is about *coordinated* motion planning. This means that we study the case of a multiple-robot system, where the robots may interfere with each other. Our work deals with a very specific aspect of coordinated motion planning: proving the optimality of motions for two robots in an obstacle-free plane (in our case, two square robots). In particular, this subject is relatively new and there are only a few works about it. In this thesis the length of a motion for two (or more) robots is the sum of the lengths of the trajectories of each robot, and so the optimal motion is the one which has the minimum length.

Most works about coordinated motion planning study problems that are different from the one that is studied in this thesis. For example, the problem of finding a path for two unlabeled robots in the plane with obstacles is studied in [8]. Moreover, in [10] it is proved that the problem is NP-hard if the number of robots is part of the input. Giving a path for two robots is much easier than finding the *optimal* one and proving that it is optimal, that's why in this thesis we deal with an obstacle-free plane. Finding short paths for a group of robots in a plane with obstacles is studied in [9]. The authors find feasible paths for a group of robots giving a performance bound of how short is the path found compared to the optimal one (they also consider the length of a motion to be the total sum of the lengths of the paths). Another example of coordinated motion planning is the problem of reconfiguring a set of labeled convex objects in an obstacle-free grid, which is treated in [2]. In that work, the goal is to find an algorithm to reconfigure a group of robots in a grid with a good time performance bound, which is more related to discrete mathematics. Finally, a very similar problem to the one of this thesis can be found in [4]. In that article the authors study the problem of moving a line segment in an obstacle-free plane. This can be seen as moving two point robots that are always at the same distance, in contrast with this thesis, in which the robots can be at any distance.

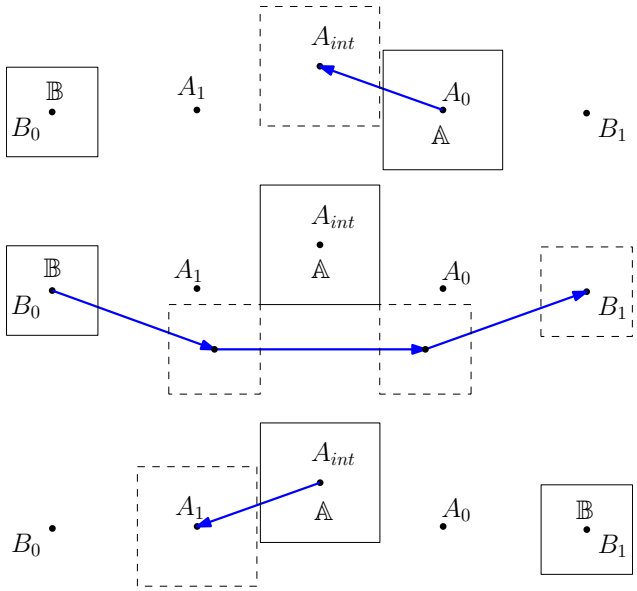

Figure 1.1: Example of optimal coordinated motion for two square robots $\mathbb{A}$ and $\mathbb{B}$, where robot $\mathbb{A}$ must go from A_0 to A_1 and robot $\mathbb{B}$ must go from B_0 to B_1. The optimal motion is as follows: 1) First, $\mathbb{A}$ is translated from A_0 to A_{int}. Mid: $\mathbb{B}$ moves from B_0 to B_1 avoiding robot $\mathbb{A}$. Bottom: $\mathbb{A}$ is translated from A_{int} to A_1.

Coordinated motion planning is much more complex that the single-robot case because the interference between the robots is a hard constraint to deal with. For example, consider the coordinated motion of Figure 1.1. As we will show in this thesis, this motion is optimal over all feasible coordinated motions for the initial and final positions A_0, B_0, A_1 and B_1. The tools used in the proof are not trivial and, as one can observe, the motion is not trivial, since we could change the point A_{int} and there is no intuitive explanation of why the point A_{int} of the example is the indicated one to get an optimal motion.

Moreover, there is the fact that we seek to find optimal motions. This is very different than finding a feasible motion (that is called pathfinding). Refer at the example (with an obstacle) of Figure 1.2. Determining a feasible motion for this example is pretty simple; first choose a path for $\mathbb{B}$ to move from B_0 to B_1 avoiding the obstacle (without moving $\mathbb{B}$). Then, first move robot $\mathbb{A}$ in the direction of the y-axis until it doesn't interfere with the path of $\mathbb{B}$. Secondly, move $\mathbb{B}$ from B_0 to B_1 along the path you chose, and finally move $\mathbb{A}$ to A_1 avoiding the obstacle.

In 2018, Dan Halperin proposed to us to read the article of Kirkpatrick and Liu [5] (and [6]) and try to generalize the results that were archieved in that work. In that article, the authors find the optimal coordinated motions for two disc robots in an obstacle-free plane. The basis of the proof is Cauchy's surface area formula (Theorem 2.13). The structure of the article is the following: first it explains the ideas behind the proof, secondly it gives a non-trivial example of optimal coordinated motion and finally it studies all the possible cases of optimal coordinated motions.

Our main goal is to find optimal coordinated motions for two squares given their final an initial positions in an obstacle-free plane. This means that every robot is located in an initial position and has to reach a final position. The unique constraint that our thesis deals with is the fact that the robots cannot collide. In this work we suppose that the squares have the same orientation and they cannot rotate. Moreover, the size of the squares may be different from each other.

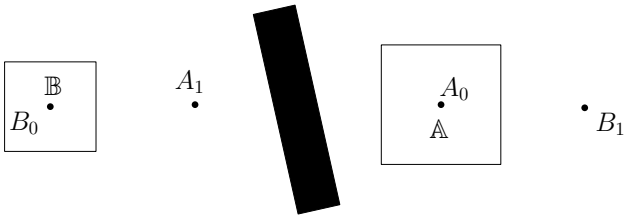

Figure 1.2: Robot $\mathbb{A}$ must go from A_0 to A_1 and robot $\mathbb{B}$ must go from B_0 to B_1. The black area is an obstacle.

The structure of this work is similar to the one of [5]; it is divided in three main chapters. In the first chapter, we introduce the basic concepts and results which are the structure behind this work and [5]. In the second chapter, we dig deeper into the case of two squares. We present new ideas and we use them to prove the optimality of a non-trivial motion for two squares. These ideas can be seen as a generalization of the ones used in [5]. To conclude, we make an exhaustive study of the possible cases of configurations and their optimal coordinated motions, which leads to our main result: we show an optimal coordinated motion for every initial and final position of two square robots and prove its optimality using the techniques presented in the second chapter. Furthermore, we show that the optimal coordinated motions follow a common logical pattern and they consist of one polygonal line for each robot.

Chapter 2

Preliminaries

In this chapter we will introduce the basic concepts of motion planning for two side-parallel square robots. They consist of an adaptation of the definitions and basic results for discs contained in [5]. We consider the robots to be open squares, which are side-parallel and they cannot rotate. Therefore, the term "robot" is used to understand the ideas of this thesis, but we will work with abstract concepts.

We refer to the two robots as $\mathbb{A}$ and $\mathbb{B}$, and generally to their positions, i.e., the positions of their centers, as A and B. The radius of a robot is defined as one half of its side. We will denote the sum of the radii of the two squares as s. This is due to the fact that the movement the robot $\mathbb{A}$ of radius s_1 in the presence of robot $\mathbb{B}$ of radius s_2 can be described as the movement of the point A in the presence of the square $\mathbb{B}'$ with center at B and radius $s = s_1 + s_2$ (see Figure 2.1). Therefore all the squares shown in the following figures will be of radius s.

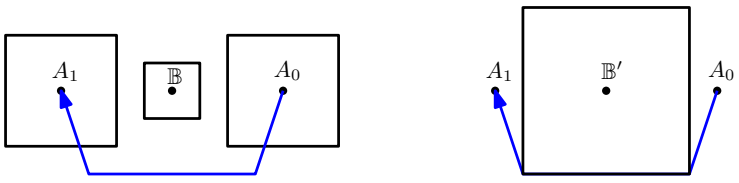

Figure 2.1: The same motion can be studied in terms of two squares of radii s_1 and s_2 (left) or in terms of a point and a square of radius $s = s_1 + s_2$ (right).

Definition 2.1. *The* position *of a square is a point in* $\mathbb{R}^2$ *defined as the location of its center. A* configuration *of a robot pair* $(\mathbb{A}, \mathbb{B})$ *is a pair of points* (A, B)*. A configuration* (A, B) *is said to be* feasible *if* $||A - B||_\infty \geq s$ *(equivalently, the two robots don't intersect each other).*

Throughout this thesis, we will denote by $P_0 = (A_0, B_0)$ the initial configuration of a robot pair, and by $P_1 = (A_1, B_1)$ its final configuration.

Definition 2.2. *A* trajectory $m_{\mathbb{A}}$ *of a robot from a position* A_0 *to a position* A_1 *is a continuous, rectifiable curve of the form* $m_{\mathbb{A}} : [0,1] \to \mathbb{R}^2$*, with* $m_{\mathbb{A}}(0) = A_0$*,* $m_{\mathbb{A}}(1) = A_1$*. A* motion m *of a robot pair* $(\mathbb{A}, \mathbb{B})$ *from a configuration* (A_0, B_0) *to a configuration* (A_1, B_1) *is a pair* $(m_{\mathbb{A}}, m_{\mathbb{B}})$*, where* $m_{\mathbb{A}}$ *is a trajectory of* $\mathbb{A}$ *from* A_0 *to* A_1 *and* $m_{\mathbb{B}}$ *is a trajectory of* $\mathbb{B}$ *from* B_0 *to* B_1*. A motion is said to be* feasible *if all the configurations* $m(t)$*,* $t \in [0,1]$ *are feasible.*

All the placements and motions that are mentioned in this thesis are aimed to be feasible.

Definition 2.3. *The* length $l(m_{\mathbb{A}})$ *of a trajectory (more generally of a curve) is the Euclidean arc-length of its trace. The* length $l(m)$ *of a motion of a robot pair* $(\mathbb{A}, \mathbb{B})$ *is the sum of the lengths of its two trajectories:*

$$l(m) = l(m_{\mathbb{A}}, m_{\mathbb{B}}) = l(m_{\mathbb{A}}) + l(m_{\mathbb{B}}).$$

Definition 2.4. *The* distance *between two configurations* $d(P_0, P_1)$ *is defined as the minimum possible length over all feasible motions from* P_0 *to* P_1*. Any feasible motion* m *between* P_0 *and* P_1 *satisfying* $l(m) = d(P_0, P_1)$ *is said to be an* optimal *motion between* P_0 *and* P_1*.*

Definition 2.5. *Let* p, q *be arbitrary points in the plane. The following definitions are illustrated in Figure 2.2:*

a) We denote by s-sq(p) *the square of radius* s *with center* p *parallel to the square robots we are considering.*

b) We denote by s-cone(p, q) *the cone formed by all half-lines from* p *that intersect* s-sq(q)*.*

c) We call support lines *from* p *to* q *the two lines that delimit the* s-cone(p, q)*. We call* support points *the intersection points of* s-sq(q) *and its support lines from* p*. In some figures the support lines will be represented as halflines.*

d) We denote by s-corr(p, q) *the* s*-corridor associated with* p *and* q*, defined as the Minkowski sum of the line segment* $\overline{pq}$ *and an open square of radius* s*.*

Next we give the basic definitions and results that we will use to find the optimal motions. Most of them are stated for $\mathbb{A}$ and $m_{\mathbb{A}}$. The definitions and results for $\mathbb{B}$ and $m_{\mathbb{B}}$ can be stated analogously.

Definition 2.6. *Let* $m = (m_{\mathbb{A}}, m_{\mathbb{B}})$ *be a motion from* P_0 *to* P_1*. We denote by* $\widehat{m_{\mathbb{A}}}$ *the closed curve defining the boundary of the convex hull of the trace of* $m_{\mathbb{A}}$*.*

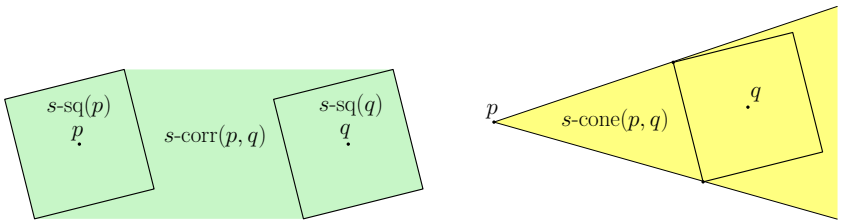

Figure 2.2: Left: example of s-corr(p, q). Right: example of s-cone(p, q).

Since $m_{\mathbb{A}}$ together with segment $\overline{A_0A_1}$ form a closed curve whose convex hull has boundary $\widehat{m_{\mathbb{A}}}$, it follows that

$$l(m_{\mathbb{A}}) \geq l(\widehat{m_{\mathbb{A}}}) - |\overline{A_0A_1}|.$$

The inequality is, in fact, an equality when the trace of $m_{\mathbb{A}}$ is convex. *When both $m_{\mathbb{A}}$ and $m_{\mathbb{B}}$ are convex, we say that m is* convex.

Definition 2.7. *The* angle of a configuration $P = (A, B)$ *is the angle formed by the vector from B to A with respect to the positive x-axis. Two points A and B are said to* be at angle θ *if the angle of $P = (A, B)$ is θ. See Figure 2.3.*

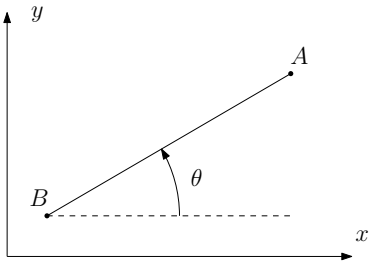

Figure 2.3: The angle θ of a configuration $P = (A, B)$.

Let $[\theta_0, \theta_1]$ be the range of angles counter-clockwise between P_0 and P_1.

Observation 2.8. *Let m be any motion from P_0 to P_1. Then m is continuous on the angles of the point configurations of $\mathbb{A}$ and $\mathbb{B}$.*

Observation 2.9. *Let m be any motion from P_0 to P_1, and let I be the range of angles realized by all the point configurations that can be realised by $\mathbb{A}$ and $\mathbb{B}$ along m. Then either $[\theta_0, \theta_1] \subseteq I$ or $S^1 - [\theta_0, \theta_1] \subseteq I$.*

Definition 2.10. *A motion m is said to be* counter-clockwise *if $[\theta_0, \theta_1] \subseteq I$.* Clockwise motions *satisfy $S^1 - [\theta_0, \theta_1] \subseteq I$.*

Observe that a motion can be clockwise and counter-clockwise at the same time, and the union of all the counter-clockwise motions and all the clockwise

ones is the total of motions. Consider the clockwise optimal motion and the counter-clockwise optimal motion for a given configuration: one of them is the optimal motion we seek to find. The following lemma gives a way to check if a counter-clockwise (or clockwise) motion is optimal.

Lemma 2.11 ([5], Observation 1.5)**.** *Let m be a (counter-)clockwise motion from P_0 to P_1 satisfying:*

1) m is convex.

2) $l(\widehat{m_{\mathbb{A}}}) + l(\widehat{m_{\mathbb{B}}})$ is minimized over all possible (counter-)clockwise motions.

Then m is a shortest (counter-)clockwise motion from P_0 to P_1.

When a counter-clockwise motion satisfies the two properties of Lemma 2.11, we say it is *counter-clockwise optimal*. The convexity of a given motion is simple to verify. In order to check the second property, the Cauchy's surface area formula is used. This formula allows to translate the problem of measuring the length of a curve into the problem of studying its support function, which, as will be seen, is an easier task.

Definition 2.12. *Let C be a closed curve. The* support function $h_C : S^1 \to \mathbb{R}$ *of C is defined as*

$$h_C(\theta) = \sup_{(x,y)\in C} \{x\cos\theta + y\sin\theta\}.$$

See Figure 2.4 left for an illustration. Given an angle θ, the points that realize the supremum are called support points*, and the line oriented at angle $\frac{\pi}{2} + \theta$ passing through the support point(s) is called* support line*.*

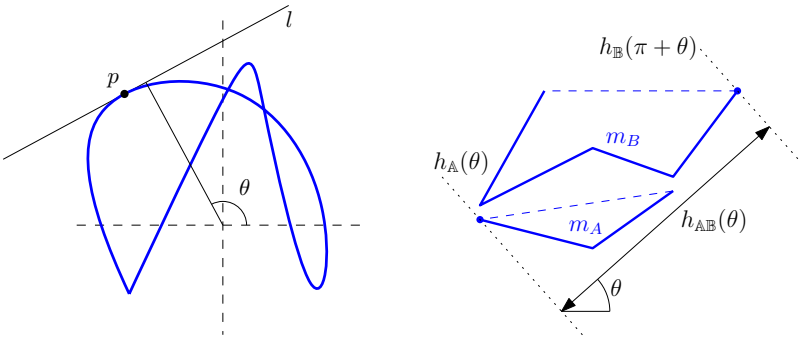

Figure 2.4: Left: Example of support point p and support line l of a closed curve. Right: Example of $h_{\mathbb{AB}}(\theta)$ of a motion. With a slight abuse of notation, the labels of $h_{\mathbb{A}}(\theta)$ and $h_{\mathbb{B}}(\pi + \theta)$ indicate the corresponding support lines.

Theorem 2.13 (Cauchy's Surface Area Formula)**.** *Let C be a closed convex curve in the plane and h_C be the support function of C. Then*

$$l(C) = \int_0^{2\pi} h_C(\theta)d\theta.$$

Corollary 2.14. *Let C_1 and C_2 be closed convex curves in the plane and let h_i be the support function of C_i. Then*

$$l(C_1) + l(C_2) = \int_0^{2\pi} (h_{C_1}(\theta) + h_{C_2}(\pi + \theta))d\theta.$$

Definition 2.15. *We denote by $h_{\mathbb{A}}$ (resp $h_{\mathbb{B}}$) the support function of $\widehat{m_{\mathbb{A}}}$ (resp $\widehat{m_{\mathbb{B}}}$). We define*

$$h_{\mathbb{AB}}(\theta) := h_{\mathbb{A}}(\theta) + h_{\mathbb{B}}(\pi + \theta).$$

This definition of support function of a motion is crucial in the main proofs of this thesis. Therefore, we are giving now another way to understand it. Given an angle $\theta \in [\theta_0, \theta_1]$, we have two support lines corresponding to it (See Figure 2.4 right for an illustration). One support line is the "caliper" perpendicular to θ enclosing $m_{\mathbb{A}}$, and the other support line is the "caliper" perpendicular to $\theta + \pi$ enclosing $m_{\mathbb{B}}$. Then $h_{\mathbb{AB}}(\theta)$ corresponds to the distance between the support lines.

In order to prove the optimality of a motion, we will first find a lower bound for $h_{\mathbb{AB}}(\theta)$. Then, for a given configuration, we will find a counter-clockwise (or clockwise) motion that matches that lower bound for every θ in the desired range of angles $[\theta_0, \theta_1]$. This will prove that the motion is optimal by Corollary 2.14: by this corollary the length of a motion is the integral of the corresponding support function $h_{\mathbb{AB}}$, therefore, if the support function is minimized then the length of the motion is the minimum and so it is optimal.

Chapter 3

Optimal motions: basics

This chapter contains the main results of this thesis. First, we will give a lower bound for $h_{\mathbb{AB}}(\theta)$ in the case of two squares, and then we will study the optimality of motions with a fundamental case, resulting in the main lemma of this thesis, which is used in every proof of the final case analysis.

3.1 Structural definitions and results

As mentioned, we seek to find a lower bound for $h_{\mathbb{AB}}(\theta)$.

In the case of two discs, giving a lower bound for it is quite simple. If s is the sum of the radii of the discs, for a given angle $\theta \in [\theta_0, \theta_1]$, we have that $h_{\mathbb{AB}}(\theta) \geq s$ independently of θ. This is due to the fact that when two disc robots are in contact, their centers stay at the same distance regardless of the angle of the configuration (see Figure 3.1, left).

This is is not so for squares, as illustrated in Figure 3.1, right. In this case, the lower bound for $h_{\mathbb{AB}}$ depends upon θ. Indeed, when two square robots are in contact, their distance depends on the angle of their configuration. This implies that the tight lower bound for $h_{\mathbb{AB}}(\theta)$ will depend upon θ. We will call it $s(\theta)$. For this reason we need to define new concepts, which will help us to better understand the construction of optimal motions.

Figure 3.1: For disc robots, as $\mathbb{A}$ slides in contact with the boundary of $\mathbb{B}$, the distance betweeen their centers stays invariable. For square robots the distance between their centers changes.

The following definitions are useful to find the desired lower bound, and they will become more clear after we see a case of an optimal motion.

Definition 3.1. *Given two points $A = (A_x, A_y)$ and $B = (B_x, B_y)$, we define the* distance between A and B at angle θ *as*

$$d_\theta(A, B) := |(A_x \cos(\theta) + A_y \sin(\theta)) + (B_x \cos(\theta + \pi) + B_y \sin(\theta + \pi))|.$$

This is a formal definition of the width of the minimum strip containing A and B with orientation θ (see Figure 3.2).

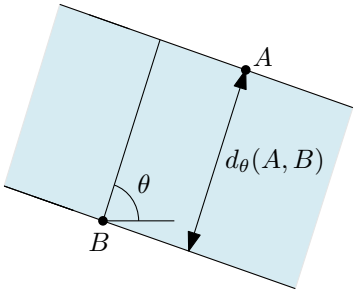

Figure 3.2: Example of $d_\theta(A, B)$.

Definition 3.2. *Let θ, θ' be two arbitrary angles. We define the* s-distance *between θ and θ' in the following way (see Figure 3.3):*

Let A, B be any two points at angle θ' such that $d_\infty(A, B) = s$, then

$$s(\theta, \theta') := d_\theta(A, B).$$

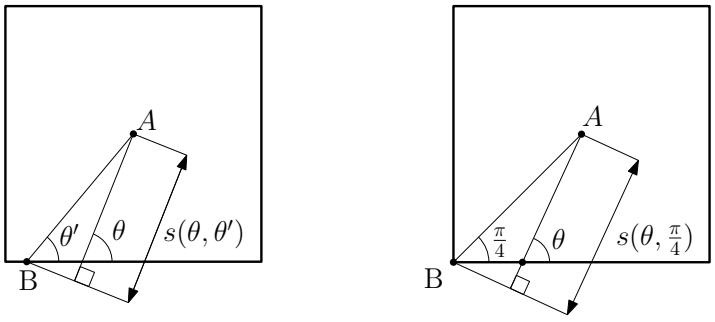

Figure 3.3: Examples of $s(\theta, \theta')$. Notice that $s\left(\theta, \frac{\pi}{4}\right) > s(\theta, \theta')$.

Definition 3.3. *Let $P = (P_0, P_1)$ be a point configuration and let $[\theta_0, \theta_1]$ be the range of angles counter-clockwise of P. We define*

$$s(\theta) := \max_{\theta' \in [\theta_0, \theta_1]} s(\theta, \theta').$$

In Proposition 3.5 we prove that function $s(\theta)$ is a lower bound for $h_{\mathbb{AB}}(\theta)$. Observe that, in the case of two disc robots, $s(\theta) = s$ for all $\theta \in S^1$, which is the lower bound for $h_{\mathbb{AB}}(\theta)$ in that case.

Now, with these definitions in mind, the following observation is immediate (see Figure 3.3).

Observation 3.4. *Given $\theta \in [0, \frac{\pi}{2}]$ (and symmetrically for the rest of angles), we have:*

$$s(\theta) = \max_{\theta' \in S^1} s(\theta, \theta') = s\left(\theta, \frac{\pi}{4}\right).$$

Grouping these new concepts together, finally arises the first important proof of our thesis. With the next proposition, we will be capable of studying the case of two squares with techniques analogous to those in [5].

Proposition 3.5. *Let $P = (P_0, P_1)$ be a point configuration and let $[\theta_0, \theta_1]$ be the range of angles counter-clockwise of P. For all counter-clockwise motions from P_0 to P_1 and $\theta \in [\theta_0, \theta_1]$, we have*

$$h_{\mathbb{AB}}(\theta) \geq s(\theta).$$

Proof. Let $\theta \in [\theta_0, \theta_1]$ and m be a counter-clockwise motion from P_0 to P_1. Since m is a counter-clockwise motion and it is continuous on the angles, there exists some configuration $(A_{\theta'}, B_{\theta'})$ of m at angle θ' for all $\theta' \in [\theta_0, \theta_1]$. Therefore, for all $\theta' \in [\theta_0, \theta_1]$,

$$h_{\mathbb{AB}}(\theta) \geq d_\theta(A_{\theta'}, B_{\theta'}) \geq s(\theta, \theta').$$

This implies that

$$h_{\mathbb{AB}}(\theta) \geq \max_{\theta' \in [\theta_0, \theta_1]} s(\theta, \theta') = s(\theta).$$

□

Observation 3.6. *Let $H_{\mathbb{A}}$ (resp $H_{\mathbb{B}}$) be the support function of segment $\overline{A_0A_1}$ (resp., $\overline{B_0B_1}$). Since $\overline{A_0A_1} \subseteq \widehat{m_{\mathbb{A}}}$ (resp., $\overline{B_0B_1} \subseteq \widehat{m_{\mathbb{B}}}$), we have that*

$$h_{\mathbb{AB}}(\theta) \geq H_{\mathbb{A}}(\theta) + H_{\mathbb{B}}(\pi + \theta).$$

Corollary 3.7. *Let $P = (P_0, P_1)$ be a point configuration, $[\theta_0, \theta_1]$ be the range of angles counter-clockwise of P, and $\theta \in [\theta_0, \theta_1]$. We have:*

$$h_{\mathbb{AB}}(\theta) \geq \max(H_{\mathbb{A}}(\theta) + H_{\mathbb{B}}(\pi + \theta), s(\theta)).$$

The way we will use this corollary is resumed in the following lemma:

Lemma 3.8. *If the support points for an angle θ of a motion are A_0 or A_1, and B_0 or B_1, then $h_{\mathbb{AB}}(\theta)$ matches its lower bound.*

Proof. Suppose that the support points for a given *theta* $\in S^1$ are A_i and B_j, for $i = 0, 1$ and $j = 0, 1$. Then, since $A_i \in \overline{A_0A_1}$ and $B_j \in \overline{B_0B_1}$, we have that $h_{\mathbb{AB}}(\theta)$ is equal to the sum of the support functions of segments $\overline{A_0A_1}$ and $\overline{B_0B_1}$, which is $H_{\mathbb{A}}(\theta) + H_{\mathbb{B}}(\pi + \theta)$. Applying Corollary 3.7, $h_{\mathbb{AB}}(\theta)$ matches its lower bound. □

3.2 Fundamental case (I): axis-aligned squares

To better understand the techniques that we will use to identify optimal motions, it is useful to study a concrete case of a non-trivial optimal counter-clockwise motion. We consider this case to be most instructive and fundamental, and it is worth to deepen in it, analogously to what is done in [5].

In this case, illustrated in Figure 3.4, B_0 and B_1 are aligned horizontally, both A_0 and A_1 lie in s-corr(B_0, B_1), and they are also symmetric with respect to the perpendicular bisector of segment $\overline{B_0B_1}$. In this situation, we can assume without loss of generality that A_0 is located closer to B_1 and A_1 lies closer to B_0.

Before describing an optimal motion for this point configuration, we define some points that are useful to prove its optimality. Refer to Figure 3.4. Let a_i be the upper support lines from A_i to s-sq(B_i), for $i = 0, 1$. These two lines intersect at A_{int}. Let b_i, for $i = 0, 1$, be the lower support lines from B_i to s-sq(A_{int}), and let C_i be the support points of b_i. By construction, a_i is parallel to b_i. Observe that a_0 is parallel to b_0 and a_1 is parallel to b_1 by construction.

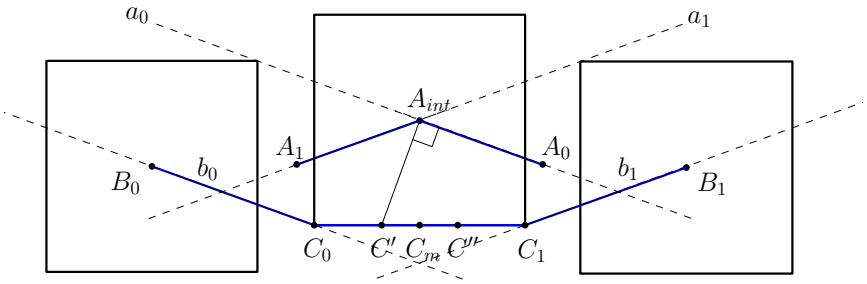

Figure 3.4: First fundamental case of a counter-clockwise optimal motion (in blue): B_0 and B_1 are aligned horizontally, and A_0 and A_1 are in their corridor.

We define C' to be the point of s-sq(A_{int}) such that segment $\overline{C'A_{int}}$ is perpendicular to a_0 and b_0, and C'' the point of s-sq A_{int} such that segment $\overline{C''A_{int}}$ is perpendicular to a_1 and b_1. Finally, we call C_m the midpoint between C_0 and C_1.

Proposition 3.9. *The following is a counter-clockwise optimal motion for the above configuration (illustrated in Figure 3.4):*

1. *Translate* $\mathbb{A}$ *from* A_0 *to* A_{int} *along* a_0.

2. *Move* $\mathbb{B}$ *from* B_0 *to* B_1 *along the shortest path avoiding* s-sq(A_{int}). *This involves translating* $\mathbb{B}$ *from* B_0 *to* C_0 *along* b_0, *sliding it along the boundary of* s-sq(A_{int}) *from* C_0 *to* C_1 *in the range of angles* $[\frac{\pi}{4}, \frac{\pi}{2} + \frac{\pi}{4}]$, *and finally translating it from* C_1 *to* B_1 *along* b_1.

3. Translate $\mathbb{A}$ from A_{int} to A_1 along a_1.

Proof. We will apply Lemma 2.11 to prove that the motion is optimal. To that end, we are going to prove that the motion is convex, and that it is minimal over all possible counter-clockwise motions.

It is obvious that the property of convexity is fulfilled (remember that a motion is convex if both paths of $\mathbb{A}$ and $\mathbb{B}$ are part of its convex hull). Next we prove that the motion is minimal, showing that $h_{\mathbb{AB}}(\theta)$ matches its lower bound. We will show that, for an angle θ, the support points are A_0 or A_1 and B_0 or B_1 (remember Lemma 3.8), or $h_{\mathbb{AB}}(\theta) = s(\theta)$.

First, when $\mathbb{A}$ moves from A_0 to A_{int} along a_0, the support points for $h_{\mathbb{A}}(\theta)$ and $h_{\mathbb{B}}(\pi + \theta)$ are A_0 and B_0, for the angles θ associated to the point configurations of this part of the motion. On the second motion, A_0 and B_0 are still the support points until $\mathbb{B}$ arrives at C'. In that moment, since a_0 and b_0 and parallel, the support points of $h_{\mathbb{A}}(\theta)$ and $h_{\mathbb{B}}(\pi + \theta)$ simultaneously become A_{int} and C_0 respectively. Then $\mathbb{B}$ moves from C' to C_m, and the range of angles associated to this part of the motion is $[\beta_0, \frac{\pi}{2}] \subseteq [\frac{\pi}{4}, \frac{\pi}{2}]$.

Let $\theta \in [\beta_0, \frac{\pi}{2}]$. By Observation 3.4, since $\frac{\pi}{4} \in [\theta_0, \theta_1]$, we have that

$$h_{\mathbb{AB}}(\theta) \geq s(\theta) = s\left(\theta, \frac{\pi}{4}\right),$$

which is the lower bound we want to match. But we observe that A_{int} and C_0 are two points at angle $\frac{\pi}{4}$, so $h_{\mathbb{AB}}(\theta) = s\left(\theta, \frac{\pi}{4}\right)$, and it matches the lower bound. By symmetry, the same works for the remaining part of the motion. This completes the proof. □

Next we generalize this argument to another fundamental case that has no analogous in [5]. The case of squares, as we have seen, is different from the case of two discs, but with the correct assumptions we will be able to reach our goal.

3.3 Fundamental case (II): arbitrary squares

In this section we deal with a case of counter-clockwise optimal motion similar to that of Section 3.2 except that now the squares are not horizontally aligned.

Using the same terminology as before, in this case there is only one contact point between $m_{\mathbb{B}}$ and s-sq(A_{int}) that we will call C. We can now state the analogous result to that of Proposition 3.9.

Proposition 3.10. *The following is a counter-clockwise optimal motion for the above configuration, illustrated in Figure 3.5:*

1. Translate $\mathbb{A}$ from A_0 to A_{int}.

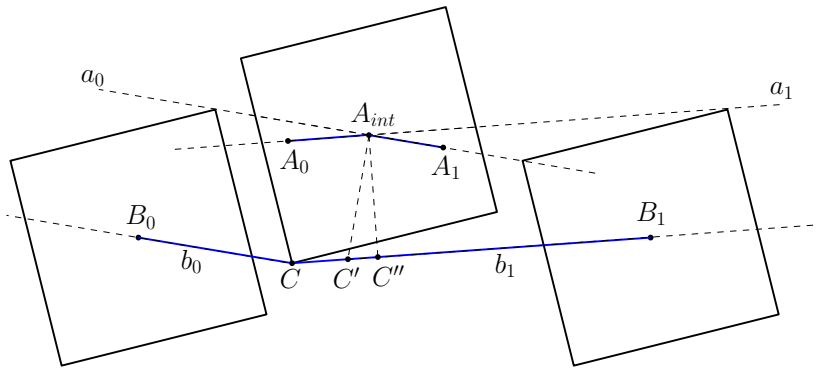

Figure 3.5: Second fundamental case of counter-clockwise optimal motion (in blue): the squares are not axis-aligned.

2. *Move* $\mathbb{B}$ *from* B_0 *to* B_1*, along the shortest path avoiding* s-sq(A_{int})*. This means translating* $\mathbb{B}$ *from* B_0 *to* C *and then from* C *to* B_1*.*

3. *Translate* $\mathbb{A}$ *from* A_{int} *to* A_1*.*

Proof. The proof is similar to that of Proposition 3.9. The differences appear on the second part of the motion, so we only discuss what happens then.

On the second part of the motion, $\mathbb{B}$ is translated from B_0 to C. Throughout this part of the motion the support points for $h_{\mathbb{A}}(\theta)$ and $h_{\mathbb{B}}(\pi+\theta)$ are A_0 and B_0. Then $\mathbb{B}$ moves from C to B_1; as before, since a_0 and b_0 are parallel, A_{int} and C simultaneously become the support points when $\mathbb{B}$ reaches point C', which is the projection of A_{int} onto b_1 in the direction perpendicular to a_0 and b_0. Finally, since a_1 and b_1 are parallel, before arriving at B_1 the support points become A_1 and B_1 simultaneously at point C'', which is the perpendicular projection of A_{int} onto b_1.

Since $\frac{\pi}{4} \in [\theta_0, \theta_1]$ and A_{int} and C are at angle $\frac{\pi}{4}$, we obtain that $h_{\mathbb{AB}}$ matches its lower bound and the motion is optimal. □

3.4 Fundamental motion

We are now ready to generalize the argument seen in the previous proofs. All of these ideas are combined together in the main lemma of this thesis. This lemma is used to prove the optimality of the motions for the general case, in Chapter 4.

Definition 3.11 (Dominated region)**.** *Let* $p \in s$-corr(B_0, B_1)*. Let* R *be the region below both upper support lines from* p *to* s-sq(B_0) *and* s-sq(B_1)*. We call* R *the* dominated region *of* p *with respect to* s-corr(B_0, B_1)*. If* $q \in R$*, we say that* p dominates q *with respect to* s-corr(B_0, B_1) *(or just* p *dominates* q*). See Figure 3.6 for an illustration.*

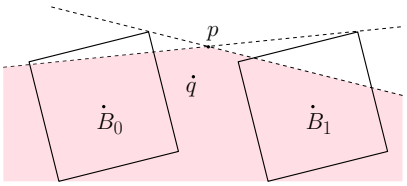

Figure 3.6: The area dominated by p is shaded. In particular, p dominates q.

Definition 3.12 (Fundamental motion)**.** *Let A_{int} be any point that dominates A_0 and A_1. A* fundamental motion *is any motion of the following form:*

1. *move $\mathbb{A}$ from A_0 to A_{int} in a motion m_1, staying entirely within the region dominated by A_{int};*

2. *move $\mathbb{B}$ on the shortest path from B_0 to B_1 that travels below s-sq(A_{int}) on a motion m_2, i.e., translate $\mathbb{B}$ along the support segment b_0 from B_0 to s-sq(A_{int}), slide it along the boundary of s-sq(A_{int}) (maybe only on one point), and finally translate it along the support segment b_1 from s-sq(A_{int}) to B_1;*

3. *move $\mathbb{A}$ from A_{int} to A_1 in a motion m_3, staying entirely within the region dominated by A_{int};*

such that:

- *m is convex;*

- *$p = A_0$, or $p = A_1$, or the tangent vectors of m_1 and m_2 at A_{int} are parallel to b_1 and b_0 respectively.*

Lemma 3.13. *(Domination lemma) In a fundamental motion, $h_{\mathbb{AB}}(\theta)$ matches its lower bound for the angles θ associated to the part of the motion in which $\mathbb{B}$ moves.*

Proof. The proof is analogous to the proofs of propositions 3.9 and 3.10. The proof needs A_{int} to dominate both A_0 and A_1 to show that the support point of $m_{\mathbb{A}}$ during m_2 is A_{int}. The parallelism condition is crucial in the previous proof. Otherwise, $h_{\mathbb{AB}}(\theta)$ fails to achieve its lower bound, as shown in Figure 3.7. Since p does not dominate A_0 (A_0 is not contained in the shaded area), when $\mathbb{B}$ moves from B_0 to C' we don't have that $h_{\mathbb{AB}}(\theta)$ matches its lower bound for that part of the motion. Moreover, since the tangent vector of m_1 at p (in the figure, segment $\overline{A_0p}$) is not parallel to b_1, when $\mathbb{B}$ moves from C' to C'' we neither have that $h_{\mathbb{AB}}(\theta) = s(\theta)$ for the angles associated to it. □

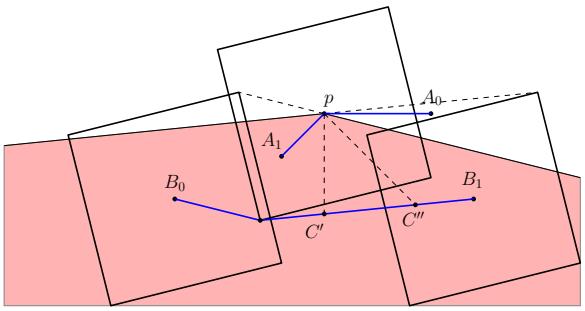

Figure 3.7: Example which does not satisfy the conditions of Lemma 3.13. The area dominated by p is shaded.

3.5 Certifying non-optimality

In some cases our method is not able to find a counter-clockwise optimal motion. This is due to the fact that the fundamental motion may be unfeasible. See Figure 3.8 for an example where the blue continuous trace corresponds to the counter-clockwise motion produced following the strategy from the previous section. Notice that it is unfeasible because it intersects the square centered at B_0.

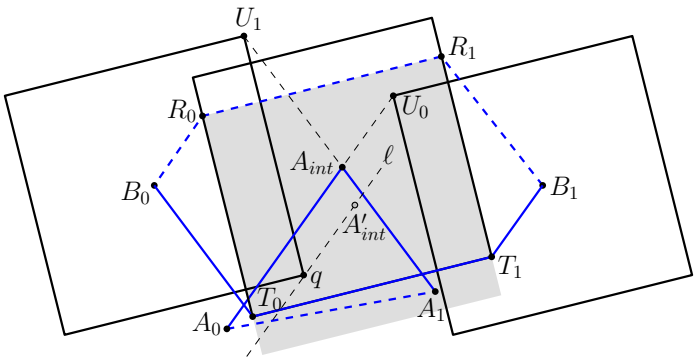

Figure 3.8: Example of a non-feasible counter-clockwise optimal motion (continuous blue trace). The dashed blue trace corresponds to m in the notation of Lemma 3.14 (case 1, when $\overline{A_0U_0}$ and $\overline{A_1U_1}$ do intersect).

In Lemma 3.14 we show that the optimal motion is clockwise for these cases. We include the proof of this lemma for completeness, although it is analogous to that of Lemma 4.6 from [5]. We will use this lemma in the following chapter to prove that the optimal motion is clockwise, instead of counter-clockwise, when the fundamental motion we give is unfeasible.

Lemma 3.14. *(Non-optimality lemma) Suppose* $A_0, A_1 \in s\text{-corr}(B_0, B_1)$. *Let* H_{ij} *denote the half-plane below the upper support line from* A_i *to* $s\text{-sq}(B_j)$. *If*

H_{ij} intersects s-sq(B_i) for $i \in \{0,1\}$, $j = 1 - i$ and $A_j \in H_{ij}$, then the optimal motion of the configuration must be clockwise.

Proof. We consider two main cases: the case where s-sq(B_0) and s-sq(B_1) do not intersect and the cases where they do intersect. In both cases, we assume that A_0 lies in the half-plane below the line connecting B_0 with B_1. The case where A_0 lies above is analogous.

Case 1: s-sq(B_0) does not intersect s-sq(B_1) (Figure 3.8). Let U_0 be the upper support point from A_0 to s-sq(B_1). By our assumptions, A_1 lies below $\overline{A_0U_0}$ and $A_1 \in s$-corr(B_0, B_1). Let U_1 be the upper support point from A_1 to s-sq(B_0). We first deal with the case where the support segments $\overline{A_0U_0}$ and $\overline{A_1U_1}$ intersect at a point $A_{int} \in s$-corr(B_0, B_1). Consider the fundamental motion m':

1. Translate $\mathbb{A}$ from A_0 to A_{int}.
2. Move $\mathbb{B}$ from B_0 to B_1 along the shortest path avoiding s-sq(A_{int}). This is done in three steps. First translate $\mathbb{B}$ to T_0, which is the lower support point from B_0 to s-sq(A_{int}). Then slide $\mathbb{B}$ counter clockwise along the boundary of s-sq(A_{int}) to T_1, which is the lower support point from B_1 to s-sq(A_{int}). This sliding is done in some range of angles $[\beta_0, \beta_1]$. Finally, translate $\mathbb{B}$ from T_1 to B_1.
3. Translate $\mathbb{A}$ from A_{int} to A_1.

The motion above is unfeasible, as A_0 cannot move from A_0 to A_{int} on a straight line without colliding with B_0. However, Lemma 3.13 shows that $l(m')$ gives a lower bound on all possible counter-clockwise motions.

Let us construct a clockwise motion whose length is no greater than that of m'. Construct the point A'_{int}, which is the result of two reflections of A_{int}, first along the line from B_0 to B_1 and then along the perpendicular bisector of $\overline{B_0B_1}$. In other words, A'_{int} is the symmetric of A_{int} with respect to the midpoint of B_0 and B_1. Consider the following motion m:

1. Move $\mathbb{B}$ from B_0 to B_1 avoiding s-sq(A'_{int}) by first translating $\mathbb{B}$ from B_0 to R_0, which is the upper support point from B_0 to s-sq(A'_{int}); then sliding it along the top boundary of s-sq(A'_{int}); and finally translating it from R_1, which is the upper support point from B_1 to s-sq(A'_{int}), to B_1.
2. Translate $\mathbb{A}$ from A_0 to A_1.

By symmetry, step 1 of m has the same length as step 2 of m'. Trivially, step 2 of m has at most the length of steps 1 and 3 of m'. Therefore, $l(m) \leq l(m')$.

Furthermore m is a feasible motion. In order to prove this, notice that the line segment $\overline{B_0R_0}$ is parallel to $\overline{A_0A_{int}}$. Consider a third line ℓ, parallel to the

two previous ones and passing through A'_{int}. Observe that s-sq(B_0) intersects ℓ in one single point q. Then, the fact that $\overline{A_0A_{int}}$ intersects s-sq(B_0) implies that A_0 does not collide with $\mathbb{B}$ when it moves from B_0 to R_0 in step 1. Hence the optimal motion must be clockwise in this case.

When the support segments $\overline{A_0U_0}$ and $\overline{A_1U_1}$ do not intersect, this means that U_1 is below $\overline{A_0U_0}$ (see Figure 3.9).

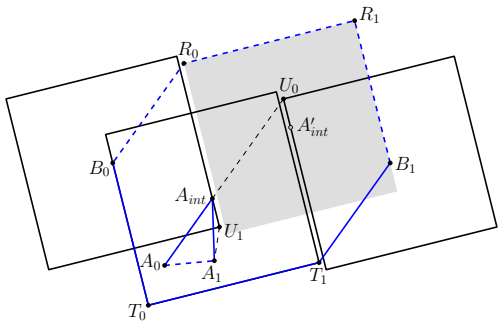

Figure 3.9: Example of a non-feasible counter-clockwise optimal motion (continuous blue trace). The dashed blue trace corresponds to m in the notation of Lemma 3.14 (case 1, when $\overline{A_0U_0}$ and $\overline{A_1U_1}$ do not intersect).

In this case, let A_{int} be the right-most intersection point between $\overline{A_0U_0}$ and s-sq(B_0). One can see that, similarly to the fundamental case studied in Section 3.3, the analogous motion m with this A_{int} gives us a lower bound of the optimal counter-clockwise length. With this, the proof above works without any modification.

Case 2: s-sq(B_0) intersects s-sq(B_1) (Figure 3.10). Let L denote the region (shaded in the figure) within s-corr(B_0, B_1) below the squares s-sq(B_0) and s-sq(B_1). We will show that if both A_0 and A_1 lie in L then the optimal motion must be clockwise. The case where they are located in the zone above the squares is handled similarly.

As before, we will first lower bound the optimal counter-clockwise motion by an unfeasible motion m', and then find a clockwise motion m whose length is at most the length of m'. We will only give both motions, the argument will be the same as before.

Let t be the upper intersection point of s-sq(B_0) and s-sq(B_1). We define A_{int} to be t and we define m' as follows:

1. Translate $\mathbb{A}$ from A_0 to A_{int}.

2. Move $\mathbb{B}$ along the shortest path from B_0 to B_1 avoiding s-sq(A_{int}).

3. Translate $\mathbb{A}$ from A_{int} to A_1.

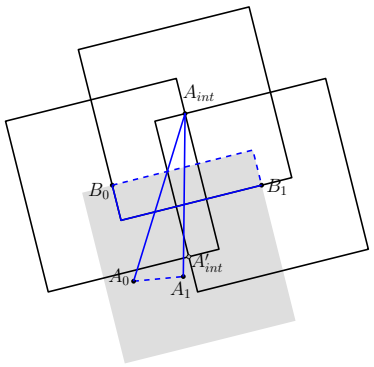

Figure 3.10: Example of a non-feasible counter-clockwise optimal motion (continuous blue trace). The dashed blue trace corresponds to m in the notation of Lemma 3.14 (case 2: s-sq(B_0) and s-sq(B_1) intersect).

Construct the point A'_{int} which is the vertical reflection of A_{int} across $\overline{B_0B_1}$. Finally we define m:

1. Move $\mathbb{B}$ from B_0 to B_1 avoiding s-sq(A'_{int}) by sliding over the top of it.
2. Move $\mathbb{A}$ on a straight line from A_0 to A_1.

□

Chapter 4

Optimal motions: general case

This chapter devoted to prove the following result, where A_{int} is defined ad-hoc for each case:

Theorem 4.1. *Given two square robots $\mathbb{A}$ and $\mathbb{B}$, with initial configurations A_0 and B_0, and final configurations A_1 and B_1, there exists a position A_{int} (exchanging the roles of $\mathbb{A}$ and $\mathbb{B}$ if required) such that the following is an optimal motion:*

1. *Move $\mathbb{A}$ along the shortest path from A_0 to A_{int} avoiding s-sq(B_0). We will call this part of the motion m_1.*

2. *Move $\mathbb{B}$ along the shortest path from B_0 to B_1 avoiding s-sq(A_{int}). We will call this part of the motion m_2.*

3. *Move $\mathbb{A}$ along the shortest path from A_{int} to A_1 avoiding s-sq(B_1). This will call this part of the motion m_3.*

In the following, we will use m to refer to a motion as described in Theorem 4.1. Without loss of generality, we may assume that B_0 and B_1 are aligned horizontally. The proof is then done by a case analysis depending on the relative positions of $\mathbb{A}$ and $\mathbb{B}$ in the initial and final configurations. For each case we fix a position for A_0, and, finally, we perform the following steps:

- We describe different zones where A_1 can be located.

- We describe the position of A_{int} for each zone.

- We prove the optimality of the resulting motion or

- we prove that the optimal motion must be the other way around (counter clockwise or clockwise) showing that the conditions of the non-optimality lemma (Lemma 3.14) are satisfied, or
- we prove that we need to exchange the roles of $\mathbb{A}$ and $\mathbb{B}$ to find the optimal motion. We give the optimal motion all the cases.

We can distinguish three major cases (not necessarily disjoint) of initial and final configurations, depending on the relative positions between the A_i's and the B_i's. Up to symmetry, exchanging the roles of $\mathbb{A}$ and $\mathbb{B}$ or exchanging the roles of A_0 by A_1 and B_0 by B_1, these cases cover all the possible situations (see Table 4.1):

- Case 1. $A_0 \notin s\text{-corr}(B_0, B_1)$ and $B_1 \notin s\text{-corr}(A_0, A_1)$.
- Case 2. $A_0 \in s\text{-corr}(B_0, B_1)$, $A_1 \in s\text{-corr}(B_0, B_1)$, $B_0 \notin s\text{-corr}(A_0, A_1)$ and $B_1 \notin s\text{-corr}(A_0, A_1)$.
- Case 3. $A_0 \in s\text{-corr}(B_0, B_1)$, $B_0 \in s\text{-corr}(A_0, A_1)$.

Then, the main subcases of cases 2 and 3 will take into account the following property:

- Subcase 1. $s\text{-sq}(B_0)$ does not intersect $s\text{-sq}(B_1)$.
- Subcase 2. $s\text{-sq}(B_0)$ intersects $s\text{-sq}(B_1)$.

	$A_0 \notin s\text{-corr}(B_0, B_1)$ $A_1 \notin s\text{-corr}(B_0, B_1)$	$A_0 \notin s\text{-corr}(B_0, B_1)$ $A_1 \in s\text{-corr}(B_0, B_1)$	$A_0 \in s\text{-corr}(B_0, B_1)$ $A_1 \notin s\text{-corr}(B_0, B_1)$	$A_0 \in s\text{-corr}(B_0, B_1)$ $A_1 \in s\text{-corr}(B_0, B_1)$
$B_0 \notin s\text{-corr}(A_0, A_1)$ $B_1 \notin s\text{-corr}(A_0, A_1)$	1	1	1	2
$B_0 \notin s\text{-corr}(A_0, A_1)$ $B_1 \in s\text{-corr}(A_0, A_1)$	1	3	1	3
$B_0 \in s\text{-corr}(A_0, A_1)$ $B_1 \notin s\text{-corr}(A_0, A_1)$	1	1	3	3
$B_0 \in s\text{-corr}(A_0, A_1)$ $B_1 \in s\text{-corr}(A_0, A_1)$	2	3	3	3

Table 4.1: All possible configurations of the A_i's and B_i's. In each cell, we distinguish the case of this chapter which covers, up to symmetry, that configuration (recall that cases 3 and 4 cover the same configurations).

4.1 Case 1

In this case, $A_0 \notin s\text{-corr}(B_0, B_1)$ and $B_1 \notin s\text{-corr}(A_0, A_1)$. Therefore, A_0 does not interfere the optimal straight-line move of $\mathbb{B}$ from B_0 to B_1 and, after that, B_1 does not interfere the straight line move of $\mathbb{A}$ from A_0 to A_1. This is a simple

case where the robot motions don't need to be coordinated. An optimal motion consists in moving first $\mathbb{B}$ on a straight line, and then moving $\mathbb{A}$ on a straight line.

4.2 Case 2

In this case, both A_0 and A_1 belong to s-corr(B_0, B_1) but none of B_0 and B_1 belong to s-corr(A_0, A_1).

Definition of the zones (Figures 4.1 and 4.2) We fix the position of A_0 and we distinguish four different zones for A_1. Let p_0 and p_1 be the upper support points from A_0 to s-sq(B_0) and s-sq(B_1) respectively.

1. Zone I is the set of points that dominate A_0.
2. Zone II is the set of points that A_0 dominates.
3. Zone III is the set of points for which the upper support line from the point to s-sq(B_0) intersects $\overline{A_0p_1}$.
4. Zone IV is the set of points for which the upper support line from the point to s-sq(B_1) intersects $\overline{A_0p_0}$.

Definition of A_{int} For each zone, we define the point A_{int}:

1. If $A_1 \in$ Zone I, then $A_{int} = A_1$.
2. If $A_1 \in$ Zone II, then $A_{int} = A_0$.
3. If $A_1 \in$ Zone III, then A_{int} is the intersection of the upper support line from A_1 to s-sq(B_0) and $\overline{A_0p_1}$.
4. If $A_1 \in$ Zone IV, then A_{int} is the intersection of the upper support line from A_1 to s-sq(B_1) and $\overline{A_0p_1}$.

4.2.1 Case 2, subcase 1: s-sq(B_0) and s-sq(B_1) do not intersect

Proof of Theorem 4.1 for this case (Figure 4.1)

- Zone I. Analogously to the fundamental case example (Section 3.3), along m_1 and m_3 the support points are A_0 or A_1 and B_0 or B_1 and we conclude that $h_{\mathbb{AB}}$ matches its lower bound m_1 and m_3 by Lemma 3.8. Since in this case $A_{int} = A_1$, m is a fundamental motion because A_1 dominates A_0 (by the definition of Zone I) and it is a convex motion. Hence we have that $h_{\mathbb{AB}}$ matches its lower bound along m_2 from Lemma 3.13. Finally, this motion is feasible since $\overline{A_0A_1}$ belongs to Zone I.

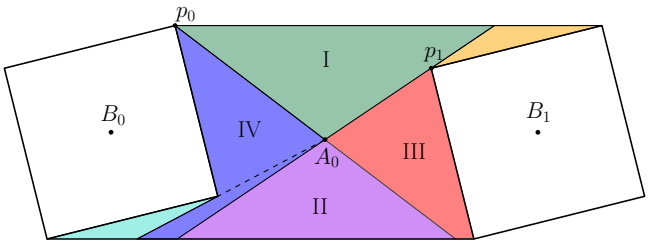

Figure 4.1: Case 2, non-intersecting case. Zone III is represented with red and orange, and Zone IV is represented with dark blue and light blue.

- Zone II. By definition $A_{int} = A_0$ dominates A_1. Taking this into account, the proof is analogous to that for Zone I.
- The red area of Zone III and the dark blue area of Zone IV are studied in Section 3.3 with the fundamental case, so the proof is exactly the same. The orange area of Zone III and the light blue area of Zone IV are studied in Case 3 (observe that those areas belong to Case 2 and Case 3).

4.2.2 Case 2, subcase 2: s-sq(B_0) and s-sq(B_1) intersect

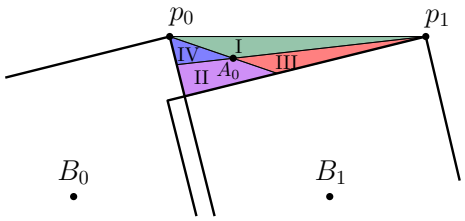

Figure 4.2: Case 2, intersecting case with A_0 above s-sq(B_0) and s-sq(B_1).

Proof of Theorem 4.1 for this case (Figure 4.2) In this subcase there are two possibilities:

- A_0 **and** A_1 **are both above** s-sq(B_0) **and** s-sq(B_1). This is the case of Figure 4.2. The optimality proof of each zone is the same as the proof of the non-intersecting case.
- A_0 **and** A_1 **are both below** s-sq(B_0) **and** s-sq(B_1). By the non-optimality lemma (Lemma 3.14) we have immediately that the optimal motion must be clockwise. Thus, by symmetry, the proof for each zone is analogous to that for the non-intersecting case but with an optimal clockwise motion. More precisely, the proof for Zone I is the same as that for Zone II of the non-intersecting case; the proof for Zone II is the same

as that for Zone I of the non-intersecting case, and the proofs for zones III and IV were studied in the fundamental case in Section 3.3.

4.3 Case 3

In this case $A_0 \in s\text{-corr}(B_0, B_1)$ and $B_0 \in s\text{-corr}(A_0, A_1)$. An important observation is that the condition of B_0 belonging to $s\text{-corr}(A_0, A_1)$ is the same as considering A_1 belonging to the part of $s\text{-cone}(A_0, B_0)$ in which segment $\overline{A_0A_1}$ intersects $s\text{-sq}(B_0)$, but we only suppose that A_1 belongs to $s\text{-cone}(A_0, B_0)$. Without loss of generality, we suppose that B_0 lies to the right A_0. For simplicity of the case analysis and to better understand it, we will look for optimal clockwise motions. This is the main and most complicated case, so we will study it in detail.

Definition of the zones (Figures 4.3, 4.4, 4.9 and 4.10) Let p be the upper support point from A_0 to $s\text{-sq}(B_0)$, and let u be the topmost point of $s\text{-sq}(B_0)$. In some cases, p and u may coincide (as in Figure 4.9). We distinguish four different zones for A_1.

I: Zone I is the set of points $q \in s\text{-cone}(A_0, B_0)$ for which some support point from $q \in s\text{-cone}(A_0, B_0)$ to $s\text{-sq}(B_1)$ lies above segment $\overline{pu}$.

II: Zone II is the set of points $q \in s\text{-cone}(A_0, B_0)$ for which the upper support line from q to $s\text{-sq}(B_1)$ intersects segment $\overline{pu}$.

III: Zone III is the set of points $q \in s\text{-cone}(A_0, B_0)$ for which the upper support line from q to $s\text{-sq}(B_1)$ intersects $\overline{A_0p}$.

IV: Zone IV is the set of points $q \in s\text{-cone}(A_0, B_0)$ that still have not been considered.

Definition of A_{int} For each zone, we define the point A_{int}:

1. If $A_1 \in$ Zone I, then $A_{int} = A_1$.
2. If $A_1 \in$ Zone II, then A_{int} is the leftmost intersection point between $s\text{-sq}(B_0)$ and the upper support line from A_1 to $s\text{-sq}(B_1)$.
3. If $A_1 \in$ Zone III, then A_{int} is the intersection point between the upper support line from A_1 to $s\text{-sq}(B_1)$ and the upper support line from A_0 to $s\text{-sq}(B_0)$.
4. Zone IV is a special case and we will handle it differently in each subcase.

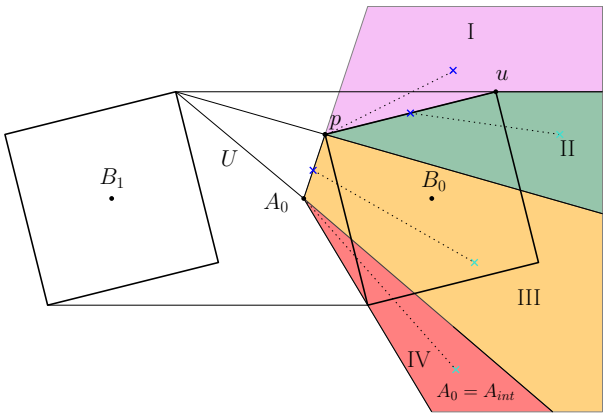

Figure 4.3: Case 3, subcase 1 with $A_0 \notin s\text{-sq}(B_1)$.

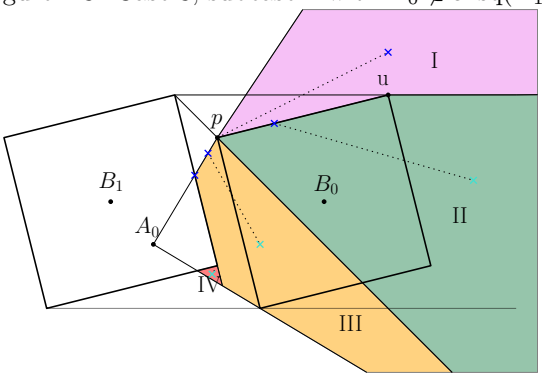

Figure 4.4: Case 3, subcase 1 with $A_0 \in s\text{-sq}(B_1)$

In figures 4.3, 4.4, 4.9 and 4.10 we show the different zones for A_1. In each zone, we give an example of the movement of $\mathbb{A}$ with a dotted polygonal line with two crossed points. The crossed points of each zone are A_{int} (painted with dark blue) and A_1 (painted with light blue). If $A_{int} = A_1$, then there is only one crossed point painted with dark blue.

4.3.1 Case 3, subcase 1: s-sq(B_0) and s-sq(B_1) do not intersect

Proof of Theorem 4.1 for this case (Figures 4.3 and 4.4)

- **Zone I**. We consider two cases depending wheter A_0 lies in s-sq(B_1) or not and, if it does not, on wheter A_1 is above or below the upper support line U from A_0 to s-sq(B_1)

  - A_1 lies above U or $A_0 \in s\text{-sq}(B_1)$ (see Figure 4.5). In this case B_0 dominates B_1 with respect to s-corr(A_0, A_1). This property is due to

two facts: A_0 belonging to s-corr(B_0, B_1) or s-sq(B_1) implies that B_1 lies above to the upper tangent from B_0 to s-sq(A_0) (we call it upper tangent taking into account that we need to consider a rotation first to make A_0 and A_1 axis-alligned). A_1 belonging to Zone I (or Zone II) implies that implies that B_1 lies above to the upper tangent from B_0 to s-sq(A_1) because A_1 lies above the upper tangent from p to s-sq(B_1).

Now we begin the proof of optimality: Exchanging the roles of $\mathbb{A}$ and $\mathbb{B}$, we define $B_{int} = B_0$. Since B_{int} dominates both B_0 and B_1 with respect to s-corr(A_0, A_1) and $B_{int} = B_0$, we obtain that m is a fundamental motion and we can apply the domination lemma 3.13 with the roles of $\mathbb{A}$ and $\mathbb{B}$ exchanged. This guarantees that $h_{\mathbb{AB}}$ matches its lower bound along m_1. Since A_1 dominates A_0 and m is trivially convex, m is a fundamental motion and we can apply the domination lemma 3.13 to obtain that $h_{\mathbb{AB}}$ matches its lower bound along m_2. since m_3 is reduced to a single point, $h_{\mathbb{AB}}$ matches its lower bound along m_3. Finally, under our assumptions, we observe that the motion m is trivially feasible.

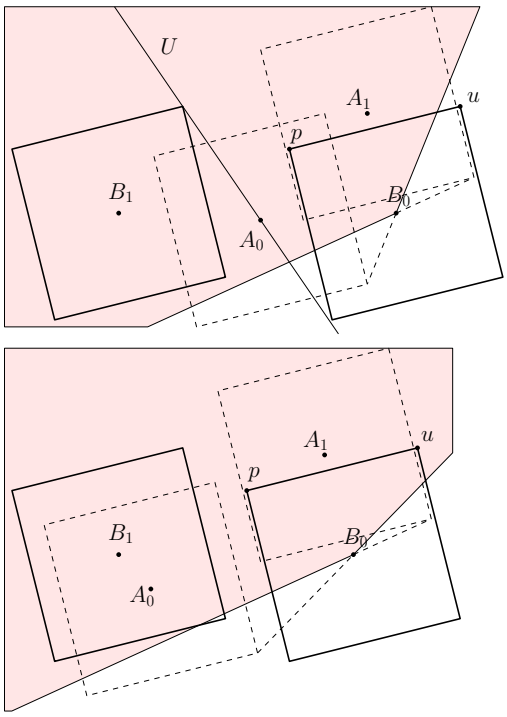

Figure 4.5: Zone I. Top: example of A_1 being above U. Bottom: example of $A_0 \in s$-sq(B_1). The shaded zones represent the domination zone of B_1 with respect to s-corr(A_0, A_1).

– A_1 lies below U and $A_0 \notin s\text{-sq}(B_1)$ (see Figure 4.6). In this case, the positions of A_0 and A_1 satisfy the conditions of the non-optimality lemma (Lemma 3.14). Thus we look for counter-clockwise motions. Rotating the configuration, in the counter-clockwise zones, A_1 is in Zone IV, which we handle below.

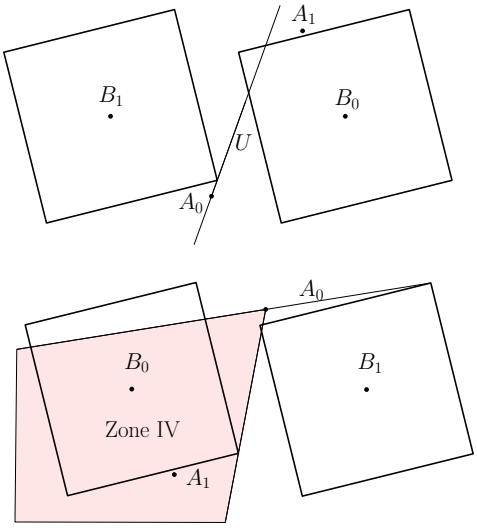

Figure 4.6: Zone I. Top: example of A_1 being below U. Bottom: The same configuration, rotated. The shaded area is Zone IV for the counter-clockwise motions.

- **Zone II**. When A_1 lies in Zone II, B_0 dominates B_1 with respect to $s\text{-corr}(A_0, A_1)$, due to the same reasons to the ones of Zone I. Therefore, defining $B_0 = B_{int}$ and applying the domination lemma 3.13 we have that $h_{\mathbb{AB}}$ matches its lower bound along m_1 since the motion is trivially convex. The same thing happens along m_2, since A_{int} dominates A_0 and A_1. Throughout m_3, the support points are A_1 and B_1 so $h_{\mathbb{AB}}$ matches its lower bound along m_3 by Lemma 3.8, and the motion is optimal since it is feasible.

- **Zone III**. The proof is analogous to that for Zone II. The only difference between these two zones is the definition of the point A_{int}. With the definition of this point for Zone III, the requirements of the proof for Zone II are also fulfilled and the proof has already been presented in Chapter 3.

- **Zone IV**. This is the most complex zone. Let p be the upper support point from A_0 to $s\text{-sq}(B_0)$ and let u be the topmost point of $s\text{-sq}(B_0)$. We distinguish three subcases depending on the positions of A_0 and A_1, and we treat each subcase in a different way:

1) (See Zone IV in Figure 4.4). $A_0 \in s\text{-sq}(B_1)$. In this case, taking A_{int} to be the intersection point of $\overline{A_0 p}$ and $s\text{-sq}(B_1)$, the same proof as the one for Zone II applies.

2) (See Figure 4.7). $A_0 \notin s\text{-sq}(B_1)$ and the upper support point of A_1 and $s\text{-sq}(B_1)$ lies inside $s\text{-corr}(B_0, B_1)$. Under these assumptions we must have $A_1 \in s\text{-corr}(B_0, B_1)$ or below the lower horizontal support line of $s\text{-sq}(B_0)$ and $s\text{-sq}(B_1)$. We prove that taking $A_{int} = A_0$ yields a clockwise optimal motion:

   By construction of Zone IV, A_0 dominates A_1 and the motion is convex. Moreover, since the upper support point of A_1 and $s\text{-sq}(B_1)$ lies inside $s\text{-corr}(B_0, B_1)$ we have that B_1 dominates B_0 with respect to $s\text{-corr}(A_0, A_1)$, thus we can apply the domination lemma twice (like in the proof for Zone II); since A_0 dominates A_1, $h_{\mathbb{AB}}$ matches its lower bound along m_2, and since B_1 dominates B_0, $h_{\mathbb{AB}}$ matches its lower bound along m_3. Recall that there is no m_1 because $A_{int} = A_0$. Therefore, the fundamental motion is optimal because under our assumptions it is feasible.

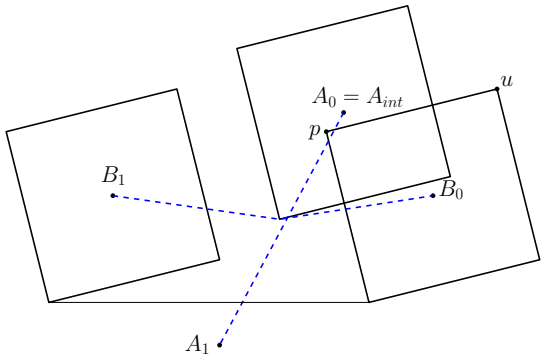

Figure 4.7: Zone IV, subcase 2 example.

3) $A_0 \notin s\text{-sq}(B_1)$ and subcase 2) does not apply. In this case A_1 must lie left of the lower support line l_1 between A_0 and $s\text{-sq}(B_1)$ (by the definition of Zone IV), above or on the lower horizontal support line from $s\text{-sq}(B_0)$ to $s\text{-sq}(B_1)$ and outside $s\text{-corr}(B_0, B_1)$ (See Figure 4.8). The hypothesis of the non-optimality lemma with the roles of $\mathbb{A}$ and $\mathbb{B}$ switched are fullfilled and the optimal motion must be counter-clockwise optimal. If we take $B_{int} = B_0$ we obtain an optimal counter-clockwise motion. This is the optimal motion of the previous subcase 2) with the roles of $\mathbb{A}$ and $\mathbb{B}$ switched.

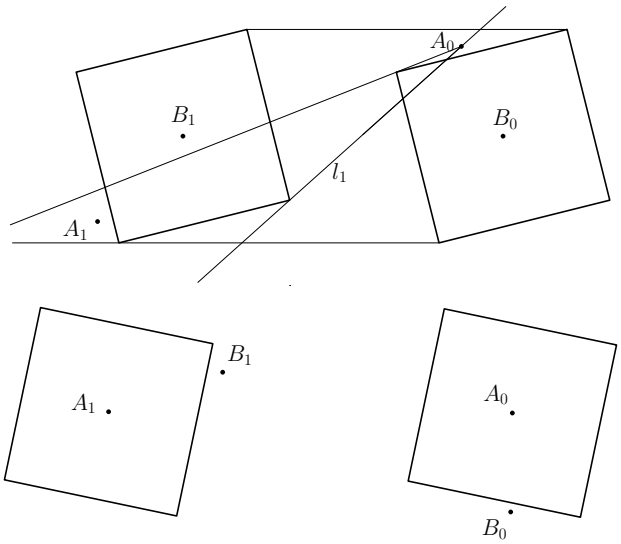

Figure 4.8: Example of Zone IV, subcase 3. The bottom configuration is the top one rotated to have A_0 and A_1 horizontally aligned. Notice how B_0 and B_1 satisfy the conditions of the non-optimality lemma.

4.3.2 Case 3, subcase 2: s-sq(B_0) and s-sq(B_1) intersect

Proof of Theorem 4.1 for this case (Figures 4.9 and 4.10)

- **Zone I**. If A_1 lies in the portion of s-cone(B_0, B_1) below s-sq(B_0) and s-sq(B_1) the fundamental motion is not feasible. But A_1 cannot lie below s-sq(B_0) and s-sq(B_1) and in Zone I at the same time, because the portion that lies below s-sq(B_0) and s-sq(B_1) is convex. Because of this convexity the support point from A_{int} to s-sq(B_1) cannot lie above segment $\overline{pu}$ (recall the definition of Zone I and the figures of the zones).

  If A_1 does not lie below s-sq(B_0) and s-sq(B_1), then the proof for Zone I in the non-intersecting case applies. This is because the zones and the point A_{int} are defined by the same properties and the property that can change is the feasibility of the fundamental motion. Therefore, the conditions of the proof are also fullfilled, like the property that A_{int} dominates A_0 and A_1.

- **Zone II**. The proof for the non-intersecting case works. This is because the feasibility of the motion does not change.

- **Zone III**. The proof for Zone II in the non-intersecting case works. This is because the feasibility of the motion does not change.

- **Zone IV**. This Zone is again the most complex one. Let p be the upper

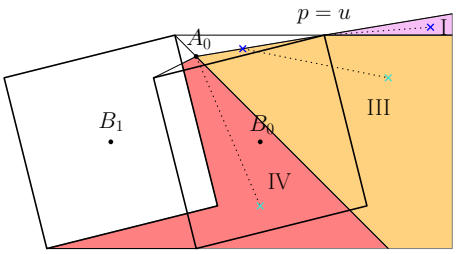

Figure 4.9: Case 3, subcase 2 with $A_0 \notin s\text{-sq}(B_1)$.

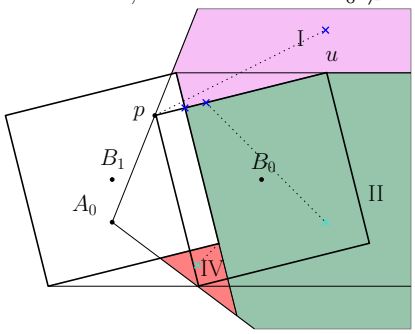

Figure 4.10: Case 3, subcase 2 with $A_0 \in s\text{-sq}(B_1)$.

support point from A_0 to s-sq(B_0) and let u be the topmost point of s-sq(B_0). We split the proof in two different subcases depending on the position of A_0:

1) A_0 lies above both s-sq(B_0) and above s-sq(B_1). In this case the motions and proofs are the same as those for the non-intersecting case for Zone IV. This is because the feasibility of the fundamental motion does not change.

2) A_0 lies below s-sq(B_0) or below s-sq(B_1). If A_1 is above of the upper support line between A_0 and s-sq(B_1) and above of the upper support line between A_0 and s-sq(B_0) (see Figure 4.11), then the non-optimality lemma shows that the optimal motion must be counter-clockwise. In this case, if we make a vertical reflection we can take $A_0 = A_{int}$ and the motion is counter-clockwise optimal since A_0 dominates A_1 with the same proof as the one in the non-intersecting case, Zone IV, 2).

   Then we assume that A_1 is outside the region handled above. In this case, as before, the proof is analogous to the one for Zone IV of the non-intersecting case with the following change: if p belongs to s-sq(B_1), we change the definition of A_{int} to be the topmost intersection point between s-sq(B_0) and s-sq(B_1). This is because if p belongs to s-sq(B_1) we need to get outside of s-sq(B_1) along

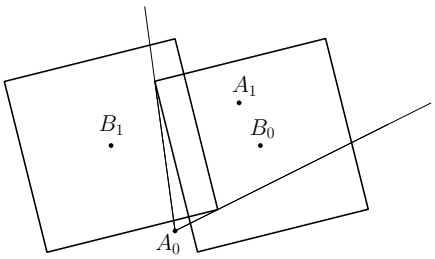

Figure 4.11: Case 3, subcase 2: Example of Zone IV, subcase 2 when the non-optimality lemma applies.

s-sq(B_0) until we reach the first point that is outside of s-sq(B_1), which is the new A_{int} (See Figure 4.12). Since p dominates A_0 and A_1 and the new A_{int} also dominates them, all the other properties of fundamental motion remain.

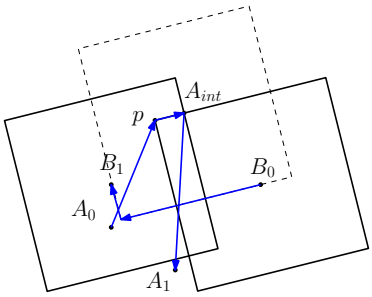

Figure 4.12: Zone IV: A_{int} is different from the non-intersecting case.

Chapter 5

Conclusions

In this work we have described and proved the optimal coordinated motions for two square robots in a obstacle-free plane. To do so, we have generalized the ideas of Kirpatrick and Liu [5] from two discs to two squares in Chapter 3. Furthermore, in Chapter 4 we have proved that the optimal coordinated motions are always polygonal lines and follow a common pattern similar to the one proved for discs [5]. Moreover, the motions can be decoupled so that only one square is moving at any given time.

The main differences between [5] and our work are:

1. The orientation of the squares matters. This doesn't happen with two discs because of their rotational symmetry.

2. We have defined the concept of $s(\theta)$ to prove a lower bound for $h_{\mathbb{AB}}(\theta)$. We need this lower bound depending on θ even when the squares are horizontally placed, which is the simplest case.

3. Lemma 3.13 (the Domination Lemma) of [5] does not hold for squares due to the orientation dependency of our problem, so we proposed a new statement that works for squares.

4. The proofs are more involved since there are more cases in the case analysis, due to the orientation dependency.

To conclude, we remark that there are many approaches and variants of this problem that are left for further research. This is a new problem and almost nothing has been done in this area, so almost all the related problems are open. The most remarkable ones are:

1. Optimal motions for other robots shapes. We have generalized the ideas for the two disc robots to two squares. The logical question now is if these new definitions and the results we have used to find optimal coordinated

motions are also valid for other shapes. For example, what happens if the robots are two equal or different convex polygons or another type of convex shapes? Furthermore, can we also find a lower bound for $h_{\mathbb{AB}}(\theta)$ and prove the optimality of a non-trivial motion?

2. Optimal motions for more than two robots. If we look for free-collision motions for three or more robots, not so much has been done. Furthermore, there are no techniques and results to show optimality of motions for three robots, and so we don't know which is the shape of these shortest motions. The algorithms that can be found are pathfinding algorithms which give computational upper bounds, but they don't say anything about the lengths of the paths and how good are they compared to the optimal ones, like in [3] and in [1].

3. Optimal motions for two robots with obstacles. Finding the optimal coordinated motion for two discs in the plane with any type of obstacle is an interesting variant of the problem. Even the case of a single point obstacle is open.

4. Optimal motions in higher dimensions. The problem of finding the optimal motion for two sphere robots in 3D space is also open.

Bibliography

[1] A. Adler, M. de Berg, D. Halperin, and K. Solovey. *Efficient Multi-robot Motion Planning for Unlabeled Discs in Simple Polygons*, pages 1–17. Springer International Publishing, Cham, 2015.

[2] E. D. Demaine, S. P. Fekete, P. Keldenich, H. Meijer, and C. Scheffer. Coordinated motion planning: Reconfiguring a swarm of labeled robots with bounded stretch. *CoRR*, abs/1801.01689, 2018.

[3] A. Dumitrescu. *Motion Planning and Reconfiguration for Systems of Multiple Objects*. 02 2007.

[4] C. Icking, G. Rote, E. Welzl, and C. Yap. Shortest paths for line segments. *Algorithmica*, 10(2):182–200, Oct 1993.

[5] D. G. Kirkpatrick and P. Liu. Characterizing minimum-length coordinated motions for two discs. In *Proc. 28th CCCG*, pages 252–259, 2016.

[6] D. G. Kirkpatrick and P. Liu. Characterizing minimum-length coordinated motions for two discs. *CoRR*, abs/1607.04005, 2016.

[7] S. M. LaValle. *Planning Algorithms*. Cambridge University Press, New York, NY, USA, 2006.

[8] M. Sharir and S. Sifrony. Coordinated motion planning for two independent robots. *Ann. Math. Artif. Intell*, 3(1):107–130, 1991.

[9] K. Solovey, J. Yu, O. Zamir, and D. Halperin. Motion planning for unlabeled discs with optimality guarantees. *CoRR*, abs/1504.05218, 2015.

[10] P. Spirakis and C. Yap. Strong np-hardness of moving many discs. *Information Processing Letters*, 19(1):55–59, 7 1984.